phys. stat. sol. (a) **183**, No. 2, 337–343 (2001)

Photorefractive Properties of CdTe:Sn

K. Shcherbin[1]) (a), V. Volkov (a), V. Rudenko (a), S. Odoulov (a), A. Borshch (a), Z. Zakharuk (b), and I. Rarenko (b)

(a) Institute of Physics, National Academy of Sciences, 03650 Kiev-39, Ukraine

(b) Department of Physics, Chernivtsy State University, Kotsyubinskogo str. 2, 58012 Chernivtsy, Ukraine

(Received July 28, 2000, in revised form September 26, 2000; accepted October 4, 2000)

Subject classification: 78.20.Ci; 78.30.Fs; S8.13

Tin is shown to be a suitable dopant that makes it possible to grow cadmium telluride crystals with considerably reduced conductivity (semi-insulating material) and ensures a well pronounced photorefractive response both for cw and Q-switched Nd^{3+}:YAG laser radiation.

1. Introduction

Semiconductor photorefractive crystals [1, 2] attract special interest of researchers because of their fast response and sensitivity in the near infrared. Cadmium telluride (CdTe) distinguishes among other photorefractive semiconductors by its high electrooptic constant $r_{123} \approx 4.5$ pm/V [3]; therefore a large two-beam coupling gain might be expected for this material [4]. In practice, however, some other important requirements should be met to ensure good photorefractive performance: (i) the crystal should possess a certain amount of donor and trap centers necessary for spatial redistribution of charges (i.e., the appropriate dopant should be added during the crystal growth) and (ii) it should be semi-insulating (to preserve a sufficient density of redistributed charges in the steady state).

Until now the photorefractive properties have been reported for vanadium-doped [5, 6], titanium-doped [5], germanium-doped [7], iron-doped [8] and vanadium-manganese codoped [9] CdTe. At the same time it is known that tin forms a deep level in the forbidden band of CdTe [10] and therefore may improve the photorefractive response. The purpose of this paper is to show that semi-insulating tin-doped cadmium telluride also exhibits remarkable photorefractive response both for cw and pulsed radiation of a 1.06 μm Nd^{3+}:YAG laser.

2. Crystal Growth and Preparation

CdTe:Sn crystals are grown in the Department of Semiconductor Microelectronics, Chernivtsy State University (Ukraine). The synthesis of cadmium telluride has been done in vacuum quartz ampoules covered with pyrolytic graphite. The vacuum distillation technique and zone refining were used to purify the initial components till at least 99.999 mass%. Tin was added in the CdTe melt with the concentration ranging from 2×10^{19} to 4×10^{19} cm^{-3}.

The ingots measuring up to 45 mm in diameter were grown by the optimized Bridgman technique in special furnaces. The dark electron conductivity dominates in the

[1]) Tel.: +380 (44) 2650818; Fax: +380 (44) 2652359; e-mail: kshcherb@iop.kiev.ua

grown crystals at ambient temperature. The X-ray diffraction was used to test the structural perfection and select the best samples.

Finally, the samples measuring $(3\ldots5)\times(4\ldots7)\times(8\ldots15)$ mm^3 are cut along the directions [110], [1$\bar{1}$0] and [001], respectively. The orientation has been done also with the X-ray control. The faces normal to [110] and [001] directions were optically finished (mechanical and chemical-mechanical treatment) and served as the input/output faces for grating recording experiments. The absorption constant α for the studied samples ranges from 0.9 to 1.4 cm^{-1}.

3. Experiments with cw Radiation

The photorefractive response of CdTe:Sn is studied with the continuous wave 1.06 μm diode-pumped single-frequency TEM_{00} neodymium YAG laser. The dozen of samples cut from three ingots are tested showing rather reproducible behaviour; the detailed study presented in what follows has been performed with the sample grown from the melt containing 2.5×10^{19} cm^{-3} of tin. A standard two-beam coupling geometry is used with two recording beams polarized normally to the plane of incidence and grating vector aligned along [001] (beam-coupling geometry for cubic photorefractive crystals [11]). The output power of the laser is up to 500 mW and the half-width of the Gaussian beams is about 3.5 mm on the sample input face.

Both the transmission grating and reflection grating geometry have been used with the grating vector always aligned along [001]. It is important to note that the efficient electro-optic constant involved in grating readout is the same for transmission as well as for reflection geometry and does not change with the angle between the recording waves.

The main characteristic measured is a beam-coupling gain factor

$$\Gamma=\frac{1}{\ell}\ln\frac{I_{\mathrm{s}}I_{\mathrm{p0}}}{I_{\mathrm{p}}I_{\mathrm{s0}}}, \tag{1}$$

where I_{s} and I_{s0} are the intensities of the transmitted signal wave in presence of the pump wave and without pump wave, I_{p} and I_{p0} are the intensities of the transmitted pump wave in presence of the signal wave and without it. The input intensity ratio of the signal to the pump wave is $I_{\mathrm{s}}/I_{\mathrm{p}}\simeq100$.

Figure 1a represents the measured dependence of the gain factor Γ versus grating spacing $\Lambda=\lambda/2\sin\theta$, where λ is the laser radiation wavelength in vacuum and θ is a half-angle between the recording waves in air. The filled dots show the data for different transmission gratings while the open dot represents the gain factor for contradirectional recording beams.

The maximum gain factor of about 0.3 cm^{-1} is reached for grating spacing slightly smaller than 1 μm thus pointing to a rather high effective trap density [12]. The solid line shows the best fit of experimental data to the calculated dependence

$$\Gamma=4\pi^2n^3r_{\mathrm{eff}}\xi k_{\mathrm{B}}T/e\Lambda\lambda(1+\ell_{\mathrm{s}}^2/\Lambda^2), \tag{2}$$

where k_{B} is the Boltzmann constant, T is the absolute temperature, n is the refractive index, e is the electron charge, ξ is the electron–hole competition factor, and the Debye screening length ℓ_{s} is given by

$$\ell_{\mathrm{s}}=\sqrt{\frac{4\pi^2\epsilon\epsilon_0k_{\mathrm{B}}T}{e^2N_{\mathrm{eff}}}}, \tag{3}$$

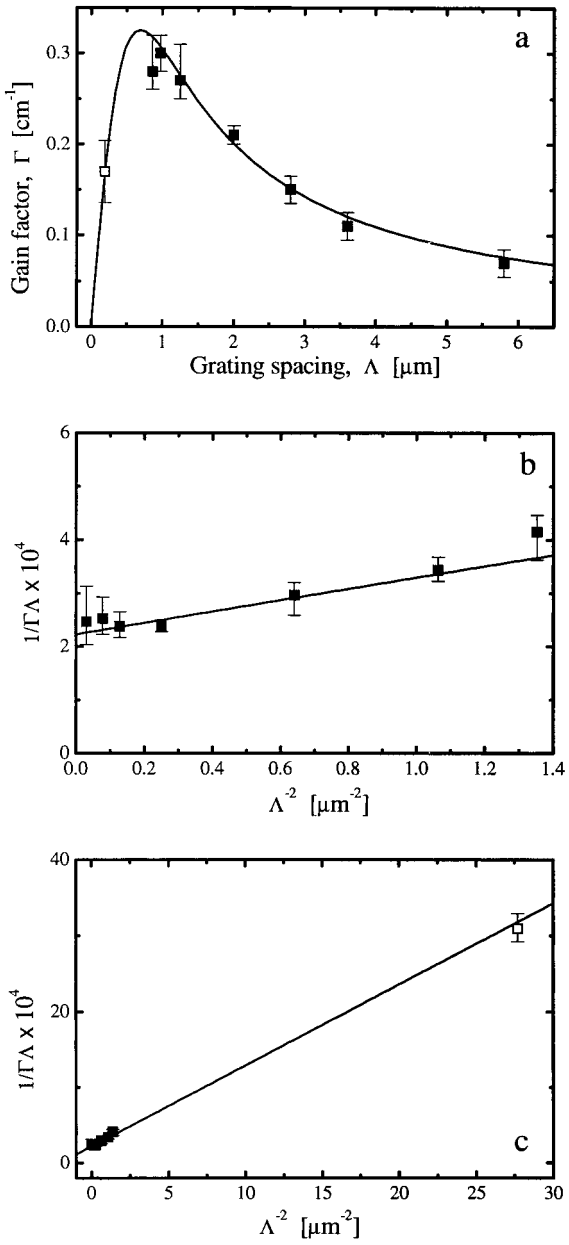

Fig. 1. a) Grating spacing dependence of the gain factor for grating recording by cw 1.06 μm radiation in CdTe:Sn; b), c) linearized dependence for evaluation of crystal parameters (see text)

with ϵ and ϵ_0 being the dielectric constants of material and vacuum, respectively, and

$$N_{\text{eff}} = N_{\text{D}}^{+}(N_{\text{D}} - N_{\text{D}}^{+})/N_{\text{D}}$$

standing for the effective trap density, N_{D} and N_{D}^{+} are the full density of donors and the density of ionized donors (traps).

Figure 1b represents the data for the transmission geometry, plotted in modified coordinates [13], aiming at linearizing the dependence and make it easier to extract the fitting parameters (Debye screening length ℓ_{s} from the slope and product ξr_{eff} from the intersection with ordinate)

$$\frac{1}{\Gamma\Lambda} = \frac{\lambda e}{4\pi^2 \xi n^3 r_{\text{eff}} k_{\text{B}} T}\,(1 + \ell_{\text{s}}^2/\Lambda^2)\,. \tag{4}$$

From the described fitting procedure the following data are extracted for the Debye screening length $\ell_{\text{s}} \approx 0.7 \pm 0.1$ μm and for the product $r_{\text{eff}}\xi \approx (2.1 \pm 0.1)$ pm/V. This enables the evaluation of the effective trap density $N_{\text{eff}} \approx 1.2 \times 10^{15}$ cm^{-3} (see Eq. (3)). Assuming that the main reason for reduction of the effective electrooptic constant as compared to its handbook value [3] is the contribution of secondary charge carriers in space charge formation [14, 15] a relevant constant of the electron–hole competition can be estimated as $\xi \approx 0.45$.

To check the correctness of the estimates extracted only from the data for the transmission geometry the full set of experimental data is presented in Fig. 1c, including the measurement for the reflection geometry. One can see that the dot for the reflection geometry is very close to the solid line which represents the best fit to the data for the transmission geometry.

4. Experiments with Pulse Radiation

A flashlamp-pumped Q-switched Nd^{3+}:YAG laser ($\lambda = 1.06$ μm, TEM_{00}, pulse duration $\tau_{pulse} \approx 20$ ns, and pulse energy $E \approx 3$ mJ) is used to study the photorefractive beam coupling with the high-power radiation. With the Gaussian beam waist about 1.6 mm the ultimate power in the sample is 3.5 MW/cm^2, i.e., at least six orders of magnitude larger than that in the experiments described in the previous section. Therefore, the dielectric relaxation time, $\tau_{di} = \epsilon\epsilon_0/\kappa I_0$ (with the dielectric constant $\epsilon\epsilon_0$, specific photoconductivity κ, and total light intensity I_0) goes down from the submillisecond range for the cw radiation to subnanosecond range for the pulsed radiation. In such a way the photorefractive grating recorded with short but powerful laser pulses is a steady-state grating and the direct comparison is possible with the data for the cw recording.

In the experiment the pulse energy is measured for the signal as well as for the pump waves. It is expected that with the grating lifetime much shorter than the pulse duration the energy is proportional to the peak intensity in each pulse and therefore an equation similar to Eq. (1) can be used for evaluation of Γ.

Figure 2 shows the dependence of the normalized energy gain $(\Delta E_s/E_{s0})^{\pm} = (E_s^{\pm} - E_{s0})/E_{s0}$ on the total pulse energy. Here E_s and E_{s0} are the energies of the transmitted pulse in presence of the second recording wave and without it, respectively. The superscripts $\pm$ denote two oposite orientations of the crystallographic axis that ensure either the amplification (+) or deplition (−) of the transmitted beam. The fringe spacing and the beam intensity ratio are kept constant in this experiment, being $\Lambda = 1.2$ μm and 25:1, respectively. The upper curve (squares) is measured for the crystal orientation when the signal wave is amplified in expense of the pump wave intensity while the lower curve is measured for the sample rotated by 180° in the plane of the input surface where the two interacting beams impinge upon the crystal. A rather strong asymmetry of two curves with respect to the line $\Delta E_s/E_{s0} = 0$ is obvious. This can be explained by the intensity dependent attenuation which occurs in addition to the beam coupling. In the first case the signal beam gain which is due to the beam coupling competes with the light-induced absorption. In the second case both processes reduce the intensity of the signal beam. Thus in addition to the photorefractive beam coupling the nonlinear absorption is observed, insensitive to the crystal orientation. We believe the two-photon absorption, which should be isotropic in the crystal of cubic symmetry,

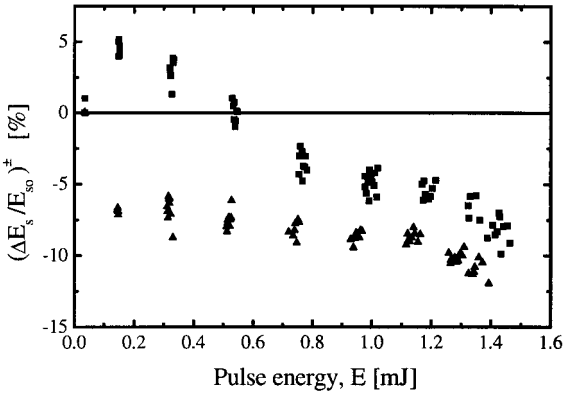

Fig. 2. Normalized energy gain $\Delta E_{s0}/E_{s0}$ versus total laser pulse energy inside the sample

is the reason of the detected depletion. The contribution of the two-photon absorption has been observed earlier in GaAs and CdTe crystals in the experiments with pulsed radiation [16, 17].

The gain factor related purely to the photorefractive beam coupling can be extracted from the data presented in Fig. 2 using the relationship

$$\Gamma = (1/2)\left[\ln\left(E_s^+/E_{s0}\right) - \ln\left(E_s^-/E_{s0}\right)\right], \tag{5}$$

with E_s^+ and E_s^- standing for the pulse energy of the transmitted signal beam amplified and depleted because of the photorefractive beam coupling.

The results of gain factor evaluation from Eq. (5) might be affected by the transient beam coupling [18] related to the free-carrier grating [19, 20]. It should be noted, however, that in the studied samples the transient beam coupling was negligibly small for pulse intensities below 3.5 MW/cm^2 .

The data presented in Fig. 2 allow to evaluate the constant β for the two-photon absorption $(\alpha \to \alpha + \beta I_0), \beta \approx (0.04 \pm 0.01)$ cm/W. This value is in a satisfactory agreement with that previously published in Ref. [21].

To estimate the gain factor Γ the maximum is chosen of the intensity redistribution in Fig. 2, to avoid strong nonlinear absorption. The grating spacing dependence of the gain factor evaluated as explained is shown in Fig. 3a. The dots show the experimental data

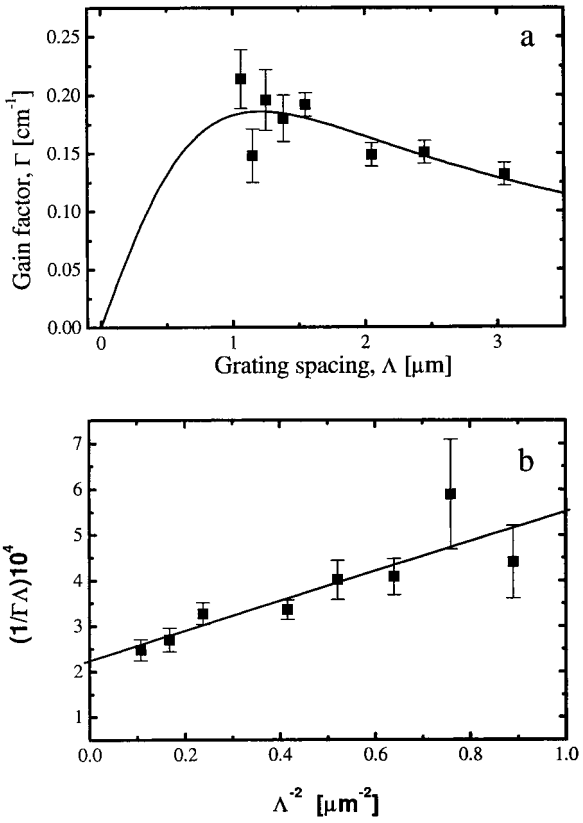

Fig. 3. a) Grating spacing dependence of the gain factor for grating recording by pulsed 1.06 μm radiation in CdTe:Sn; b) linearized dependence for evaluation of crystal parameters (see text)

while the solid curve is again the least square fit to Eq. (2). When comparing to Fig. 1a one can see that the ultimate value of the gain factor is reduced approximately 1.5 times and the maximum is shifted to larger Λ thus pointing to the smaller effective trap density.

In Fig. 3b the same data are shown in modified coordinates [13], in similar way as it has been done for the cw recording (Fig. 1b). The extracted data are $\ell_s \approx (1.2 \pm 0.2)$ μm for the Debye screening length ($N_D \simeq 0.4 \times 10^{15}\text{cm}^{-3}$) and $\xi r_{\text{eff}} \approx (2.1 \pm 0.1)$ pm/V.

5. Discussion

The comparison of the data measured with cw and with pulsed radiation show not too high but well detectable difference. It is not unexpected because of the very important difference in light fluxes. One can imagine that with the megawatt intensities of light the density of photoexcited free carriers may become not negligible compared to the densities of the defect and impurity centers involved in the photorefraction. This guess is justified by early observation of the free-carrier holograms in CdTe [20] that can be detected only for high density of electron–hole pairs. Thus, the decrease of the effective trap density looks reasonable.

The other factor that can lead to the distinction is the electron–hole competition in the grating formation. The saturation intensities for excitation of electrons and excitation of holes are, most probably, not the same. Thus it is not excluded that for certain intermediate intensity the excitation of carriers of one sign will be nearly saturated while the excitation of carriers of opposite sign will still be linear in intensity [22]. This will certainly affect the electron–hole competition constant ξ. We do not know at present the sign of main photoexcited carriers in CdTe:Sn but judging from the values of ξ quite different from ± 1, the conclusion can be made about a rather strong contribution of both photoexcited holes and photoexcited electrons to the grating formation.

6. Conclusions

The gain factor up to 0.4 cm^{-1} is reached with cw radiation and 0.22 cm^{-1} with pulsed radiation. In previous experimental sections we restricted ourselves by the description of the data for only one selected sample. It should be underlined that similar data were obtained also for eleven other samples cut from different parts of the same and two other CdTe:Sn ingots. We do observe differences in absolute measured values of the gain factor but the spread of data is not exceeding 30% from sample to sample. The better data for the gain factor have been reported for cadmium telluride with other dopants, e.g., for CdTe:Ge, but with much stronger dispersion from sample to sample. A rather good reproducibility of the results is an obvious advantage of tin-doped CdTe.

Acknowledgements

The financial support of the Science and Technology Center, Ukraine (STCU) is gratefully acknowledged. We are thankful for valuable suggestions of the reviewer of this paper.

References

[1] M. B. KLEIN, Opt. Lett. **44**, 350 (1984).
[2] A. M. GLASS, A. M. JOHNSON, D. H. OLSON, W. SIMPSON, and A. A. BALLMAN, Appl. Phys. Lett. **44**, 948 (1984).

[3] K. Tada and M. Aoki, Jpn. J. Appl. Phys. **10**, 998 (1971).
[4] V. Vinetskii, N. Kukhtarev, S. Odoulov, and M. Soskin, USSR Invention Certificate No. 603276, class G03H1/00, December 21, 1977, in: Bull. of Invention No. 43, 250 (1978).
[5] R. B. Bylsma, P. M. Bridenbaugh, D. H. Olson, and A. M. Glass, Appl. Phys. Lett. **51**, 889 (1987).
[6] L. A. de Montmorillon, Ph. Delaye, G. Roosen, H. Bou Rjeily, F. Ramaz, B. Briat, J. G. Gies, J. P. Zielinger, M. Tapiero, H. J. von Bardeleben, T. Arnoux, and J.-C. Launay, J. Opt. Soc. Am. B **13**, 2341 (1996).
[7] K. Shcherbin, A. Shumeljuk, S. Odoulov, P. Fochuk, and G. Brost, Proc. SPIE **2795**, 236 (1996).
[8] V. Volkov, A. Borshch, M. Brodyn, and V. Rudenko, Proc. SPIE **3294**, 115 (1998).
[9] R. N. Schwartz, Chen-Chia Wang, S. Trivedi, G. V. Jagannathan, F. M. Davidson, Ph. R. Boyd, and U. Lee, Phys. Rev. B **55**, 15378 (1997).
[10] W. Jantsch and G. Hendorfer, J. Cryst. Growth, **101**, 404 (1990).
[11] J. C. Fabre, J. M. C. Jonathan, and G. Roosen, Opt. Commun. **64**, 257 (1988).
[12] N. Kukhtarev, V. Markov, S. Odoulov, M. Soskin, and V. Vinetskii, Ferroelectrics **22**, 949 (1969).
[13] M. B. Klein and G. C. Valley, J. Appl. Phys. **57**, 4901 (1987).
[14] E. Strohkendl, J. Jonathan, and R. Hellwarth, Opt. Lett. **11**, 312 (1986).
[15] M. C. Bashaw, T.-P. Ma, and R. C. Barker, J. Opt. Soc. Am. B **9**, 1666 (1992).
[16] G. C. Valley, A. L. Smirl, M. B. Klein, K. Bohnert, and T. F. Boggers, Opt. Lett. **11**, 647 (1986).
[17] A. A. Borshch, M. S. Brodyn, O. M. Burin, V. I. Volkov, N. V. Kukhtarev, T. I. Semenets, and Z. N. Smereka, Sov. J. Quantum Electron. **20**, 837 (1990).
[18] V. L. Vinetskii, N. V. Kukhtarev, and M. S. Soskin, Sov. J. Quantum Electron. **7**, 230 (1977).
[19] H. J. Eichler, P. Günter, and D. Pohl, Laser-Induced Dynamic Gratings, Springer Optical Sci., Vol. 60, Springer-Verlag, Heidelberg/Berlin 1986.
[20] V. Kremenitskii, S. Odoulov, and M. Soskin, phys. stat. sol. (a) **51**, K63 (1979).
[21] E. W. Van Styrland, M. A. Woodall, H. Vanherzeele, and M. J. Soileau, Opt. Lett. **10**, 490 (1985).
[22] N. Barry and M. J. Damzen, J. Opt. Soc. Am. B **9**, 1488 (1992).